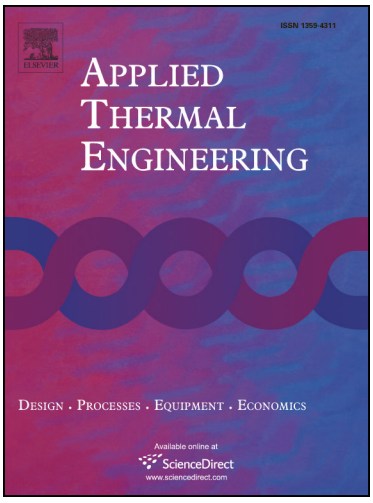

An Experimental investigation on the effect of NEW continuous core-baffle geometry on the mixed convection heat transfer in shell and coil heat exchanger

R. Andrzejczyk, T. Muszynski

PII: S1359-4311(17)36117-3
DOI: https://doi.org/10.1016/j.applthermaleng.2018.03.003
Reference: ATE 11891

To appear in: *Applied Thermal Engineering*

Received Date: 21 September 2017
Revised Date: 26 February 2018
Accepted Date: 1 March 2018

Please cite this article as: R. Andrzejczyk, T. Muszynski, An Experimental investigation on the effect of NEW continuous core-baffle geometry on the mixed convection heat transfer in shell and coil heat exchanger, *Applied Thermal Engineering* (2018), doi: https://doi.org/10.1016/j.applthermaleng.2018.03.003

AN EXPERIMENTAL INVESTIGATION ON THE EFFECT OF NEW CONTINUOUS CORE-BAFFLE GEOMETRY ON THE MIXED CONVECTION HEAT TRANSFER IN SHELL AND COIL HEAT EXCHANGER

R. Andrzejczyk [1], T. Muszynski [1]
[1]Gdansk University of Technology
Narutowicza 11/12, 80-233 –Poland

Keywords: heat transfer enhancement, shell and coil heat exchanger, heat transfer coefficient, Nusselt Number

Abstract

In the article, the authors presented the influence of continuous core-baffle geometry at mixed convection heat transfer in shell and coil heat exchanger. Experiments were carried out for a large power range, i.e. from 100W to 1200W and mass flow rates ranging from 0.01 kg/s to 0.025 kg/s. During the experiments, the mass flow rate of cooling water, the temperature of water at the inlet and outlet as well as the wall temperature of the coil (at 6 points over the coil's circumference) and the water temperature in the jacket of the exchanger (at 10 points along the shell height) were measured. The article confirmed that new form of continuous baffle geometry can successfully enhance heat transfer, but rather for small values of mass flow rates. It was also noted that the inlet/outlet configuration has significant influences on the fluid flow as well as temperature distribution at the jacket of the heat exchanger. The new experimental Nusselt numbers correlation at the shell side of the heat exchanger with continuous core-baffles was presented.

Nomenclature

A surface area, m^2,
B outside diameter of inner cylinder, m,
C inner shell diameter, m,
c_p specific heat, J/kgK
D_0 coil diameter, m
De Dean number,
D_H coil annulus diameter, m
f friction factor
G mass flow rate, kg/m^2s,
H height, m
i number of consecutive measurement,
I current, A,
k dimensionless pitch ratio (coil torsion) = $p/\pi d\delta$
L coil length, m,
$LMTD$ –logarithmic mean temperature, K
$\dot{m}$ mass fux, kg/s
n number of computational regions,
N number of baffle coils,
Nu Nusselt number,
p distance between consecutive coil turns, m,
PF – performance factor,
Pr Prandtl number,
ΔP total pressure drop, Pa,
$\dot{Q}$ heat flux, W,
q heat flux density, W/m^2,
r radius, m,
Ra Rayleigh number,
Re Reynolds number,
Ri Richardson number,
T Temperature, K,
U voltage ,V,
V volume, m^3,

Greek symbols

α heat transfer coefficient, W/m^2K,
β coefficient of thermal expansion, 1/K
δ curvature ratio, -
λ thermal conductivity, W/mK,
μ dynamic viscosity, Pas,

Subscripts

a ambient,
av average value,
b baffle,
el electric,
H helis,
i local value,
in inlet,
o outer,
out outlet,
r reference
s surface,
shw shell side wall,
sh shell side,
w water,

Abbreviations

SCHX shell coil heat exchanger,
HCT helically coiled tube,
HX heat exchanger,

1. Introduction

One of the main advantages of shell and coil heat exchangers (SCHX) is a highly efficient use of space. They are also one of the simplest design, to produce and low-cost equipment [1,2]. Due to that fact, the helical coil heat exchangers are still very common in chemical, food industries, heating ventilating and air-conditioning and heat pump applications. Though there are numerous works describing heat transfer at coil side of shell and coil heat exchanger, not many investigate shell side mixed convection [3]. Meanwhile, the conventional construction of such equipment under low fluid flow rates of fluid at shell side have low heat-transfer coefficients and are becoming uneconomical [4]. Such flow parameters are very common in many industrial applications, especially in hot water production and solar energy utilization. For this reason, there is still a great need to enhance heat transfer in coiled pipes [5]. Generally, there are two concepts to enhance the heat transfer, the active [6] and the passive methods [7]. These techniques are widely used to reduce heat exchangers weight and size or enhance their performance [8]. Prediction of the heat transfer [9,10] and pressure drop [11,12] is of primary importance for numerous applications [13,14]. There are plenty of works regarding passive and active techniques for increasing heat transfer coefficient rather in straight tubes [15]. The most popular passive techniques are twisted tape inserts, helical wire insert, swirl generators, swirl conical ring and ribs [16]. It is also worth noting, that so far in most of the literature studies the vortex and swirl generator promoted heat transfer significantly while reporting large pressure drops. A good example of new geometry with gives the opportunity to enhancement heat transfer and provide low-pressure drops was reported in [17,18]. However, heat transfer intensification techniques are not common in the case of shell coil heat exchangers.

Acharya et al. [19] investigated the concept of chaotic mixing, as a perspective technique to increase the performance of coiled tube heat exchangers. They found that it could enhance heat transfer in the range 7% - 20% in terms of the fully developed Nusselt number with little change in the pressure drop. Naphon [20] presented experimental results for helically coiled tube heat exchanger and for helically coiled finned tube heat exchanger. The effectiveness of finned tube heat exchanger is proved to be greater, 0.95 compared to 0.8 effectiveness for plain coiled tube heat exchanger. Yildiz et al. [21] in their work presented the possibility to use both passive and active techniques to enhance heat transfer in coiled tube heat exchangers. They studied the effect of the rotation of helical pipes on the heat transfer rates and pressure drops for various air-flow rates. They noted that although this technique increases pressure drop over 500% , it also augments heat transfer about 250%. The authors in their next study [22] presented heat exchanger (HX) constructed by placing spring shaped wire with varying pitch into the coil. They observed that the helical spring elements enhanced heat transfer ~ 30% but also increase in pressure losses, even as high as 1000%. Their results indicated that the Nusselt number increased with decreasing wire to pitch diameter ratio. Thomas et al. [23] experimentally and numerically investigated the performance of heat transfer in helically coiled tube heat exchanger with wire coil inserts. The studies were carried out for varying pitches and identical diameter of inserted wires in the coiled heat exchanger. The effect of the pitch of the coil wire insert on the heat transfer was studied experimentally for different Reynolds numbers of the fluid inside the coiled tube ranging from 7000 to 28000. The experiments were performed with three different pitches. All the coils were having the same cross-sectional areas. Further, the heat transfer in helically coiled heat exchanger was simulated by varying the coil pitches and at different fluid using

ANSYS software. The experimental results showed that the use of wire coil inserts leads up to 30% enhancement in heat transfer rate. Panahi and Zamzamian [24] presented the fabrication method of the helically coiled tube which contains turbulator, along with the effects of turbulator on thermal and frictional characteristics of the heat exchanger. Experiments were performed with water and air as working fluids inside the coil. At shell side, the working fluid was always hot water. Experiments were performed for both empty coiled tube and with vortex generator under different fluid flow rates. Findings showed that this type of turbulator can be employed in coiled tubes which increased the overall heat transfer coefficient up to 50% and pressure drop up to 400%.

Next challenge is the fact that most studies on helical tubes have been carried out for the heat transfer characteristics of the fluid flowing inside the helical tubes. Only a few papers concentrated on heat transfer at shell side in the helical heat exchanger. Avina [25] in his study has suggested, that because of lack of correlations for the heat transfer associated with the forced flow over helical tubes, the Zukauskas correlation can be used for the heat transfer estimation. However, the author also noted that use of this model can increase uncertainty. Authors also stated that more inaccuracy may occur because flow over the helical coils will be of a different nature than flow over tubes in cross flow. Kharat et al.[26] developed a new correlation for heat transfer coefficient for flow between concentric helical coils. This correlation was found to yield discrepancies with the increase of the distance between the concentric coils when compared with the experimental results. The experimental data and CFD simulations using Fluent were used to develop improved heat transfer coefficient correlation for the flue gas side of heat exchanger. Optimization was done using numerical technique and it is found that the new correlation for heat transfer coefficient developed in

this investigation provides an accurate fit to the experimental results within 3–4% error band. Mianroudi [3] experimentally studied mixed convection heat transfer in a shell-coil heat exchanger for various Reynolds numbers, various tube-to-coil diameter ratios, and different dimensionless coil pitch. The experiments were conducted for both laminar and turbulent flows in the coil. Effects of coil pitch and tube diameter on shell-side heat transfer coefficient of the heat exchanger were studied. Different characteristic lengths were used in various Nusselt number calculations to determine which parameter best fits the data and several equations were proposed. The results indicate that the equivalent diameter of the shell is the best characteristic length. Authors presented their own experimental correlation for shell side Nusselt number, see equation (1).

$$Nu = 0.0041 \cdot Ra^{0.4533} \cdot Re^{0.2} \cdot Pr^{0.3} \quad (1)$$

where 120 < Re< 1200, $1.2*10^7$< Ra < $3.2*10^8$.

Salem et al. [27] experimentally investigated the characteristics of convective heat transfer in horizontal shell and coil heat exchangers in addition to friction factor for fully developed flow through the helically coiled tube (HCT). Five constructions of heat exchangers with different HCT-curvature ratios (d) and tested at different mass flow rates and inlet temperatures of the two sides of the heat exchangers. Results showed that the average Nusselt numbers of the two sides of the heat exchangers and the overall heat transfer coefficients increased by increasing coil curvature ratio. The average increase in the average Nusselt number is of 160.3–80.6% for the HCT side and of 224.3–92.6% for the shell side when d increases from 0.0392 to 0.1194 within the investigated ranges of different parameters. Also, for the same flow rate in both heat exchanger sides, the effect of coil pitch and number of turns with the same coil torsion and tube length is remarkable on shell average Nusselt number while it is insignificant

on the HCT-average Nusselt number. In addition, a significant increase of 33.2–7.7% is obtained in the HCT-Fanning friction factor (fc) when d increases from 0.0392 to 0.1194. The correlation for the average Nusselt numbers for shell side as a function of the investigated parameters are obtained, equation (2). Equation (2) is applicable for 179 < Resh <1384, 5:25 <Prsh <7:54, and 0:0392 < d < 0:1194 with maximum deviation of 15%.

$$Nu = 4.4275 \cdot Re^{0.4922} \cdot Pr^{1.5676} \cdot \delta^{0.6964} \quad (2)$$

Mahdi et al. [28] experimentally and numerically investigated heat transfer enhancement in the shell and coil heat exchanger. Thre helical coil tube heat exchangers with different curvature ratio (D/d) 12/1, 15/1, 17/1, 20/1 and 24/1 were studied. Four helical coils with different coil pitch 1.8d, 2d, 3d, and 5d were selected to study the effect of coil pitch on heat transfer coefficient. From experimental results, the curvature ratio 17/1 gives optimal geometry. Experimental results show increases in coil pitch lead to increase in heat transfer coefficient of the shell side and indicate that convective heat transfer is increased by Reynolds number as well as Dean Number. The new correlation for shell side Nusselt number was obtained. The authors emphasize that empirical correlation has good agreement with experimental data and numerical results, see equation (3). Equation (3) is applicable for 500 ≤ De ≤ 1500 and 3.5<Pr<5.5.

$$Nu = 0.31 \cdot De^{0.6323} \cdot Pr^{0.28} \quad (3)$$

Salem et al. [27] presented in their work an experimental study of the horizontal shell and coil heat exchangers. Characteristics of the convective heat transfer in this type of heat exchangers and the friction factor for fully developed flow through their helically coiled tube (HCT) were investigated. Here, five heat exchangers of counterflow configurations were constructed with

different HCT torsions (k) and tested at different mass flow rates and inlet temperatures of both sides of the heat exchangers. In total, 295 test runs were performed from which the HCT-side and shell-side heat transfer coefficients were calculated. Results showed that the average Nusselt numbers of both sides of the heat exchangers and the overall heat transfer coefficient increase by decreasing coil torsion. From the test runs that were performed for the shell side, a correlation to estimate Nusselt number was obtained as follows:

$$Nu = 0.17134 \cdot Re^{0.5009} \cdot Pr^{1.4573} \cdot k^{-0.5919} \quad (4)$$

Equation (4) is applicable for 180 < Re_{sh} <1383, 5:36< Pr< 7:52, and 0:0442 <k <0:1348 with maximum deviation of 12.3%.

Objectives

Although some information is currently available on the enhancement techniques for shell coil heat exchanger most of them focused on intensification of coil side heat transfer coefficient. So there is still plenty room to discuss the enhancement techniques for shell side in this type of heat exchangers. Following the work reported in [29,30], the primary objective of the present study is to provide a comprehensive experimental database for new baffle geometry for steady state conditions. The gathered database will allow to:

(1) Obtain temperature profiles of water on the shell side of the heat exchanger.

(2) Recognize the effect of heat flux on heat transfer coefficients.

(3) Recognize the effect of buoyancy on conjugated heat transfer.

(4) Recognize the effect of new baffle geometry at pressure drops characteristics

(5) Confirm the possibility of intensifying heat exchange in the shell coil heat exchanger using a special design of baffles.

(6) Validate ability of selected experimental correlations to predict heat transfer coefficients at shell side of shell coil heat exchanger

2. Experimental setup

In the experimental studies modified version of the module, was used. The main difference is the fact that new element has been equipped with series of thermocouples (type J) to measure of shell water temperature distribution, see Fig.1. Six thermocouples were welded to the heater surface and also the ten of thermocouples was placed along the flow path line. All thermocouples were calibrated in the ultra-thermostatic bath.

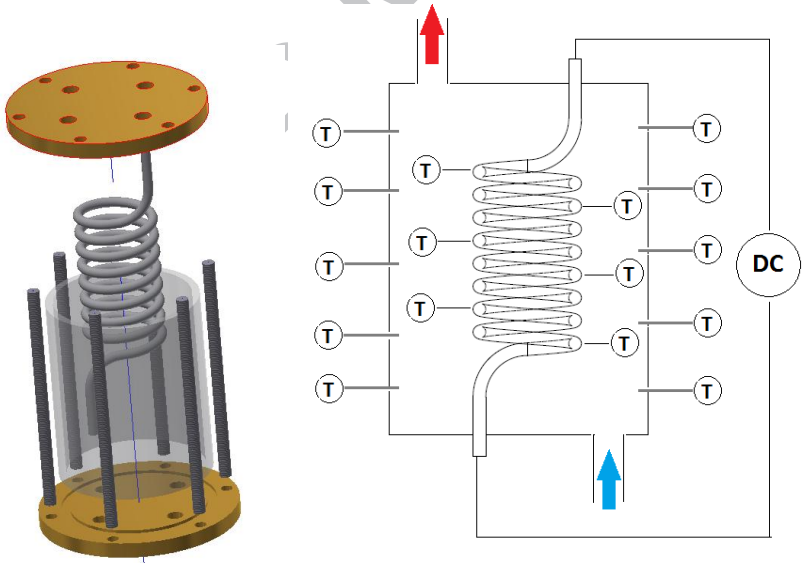

Fig.1 Experimental testing module: at left construction of the helical coil experimental module; at right temperature sensor distribution [29]

The biggest advantage of presented assembly is a possibility to change immersion depth of all of the temperature sensors. The coil was created from an electric heater with maximum electric power 1400 W. The geometry of this element was the same as in the

previous study [29] (length 1.4 m and outer diameter 6.4 mm). This element was bent to the desired shape by use of a lathe. As for the shell geometry itself, the core was fastened in the center of the bottom manifold, it resulted in reduced space at shell side of HX, thus increasing local fluid velocity. Also, the new continuous baffle geometry was applied. It is important to emphasize that in this HX geometry length of baffle gap was limited by core inside the shell. The new shell coil HX geometry is presented in Fig.2, while its geometrical parameters are presented in table 1.

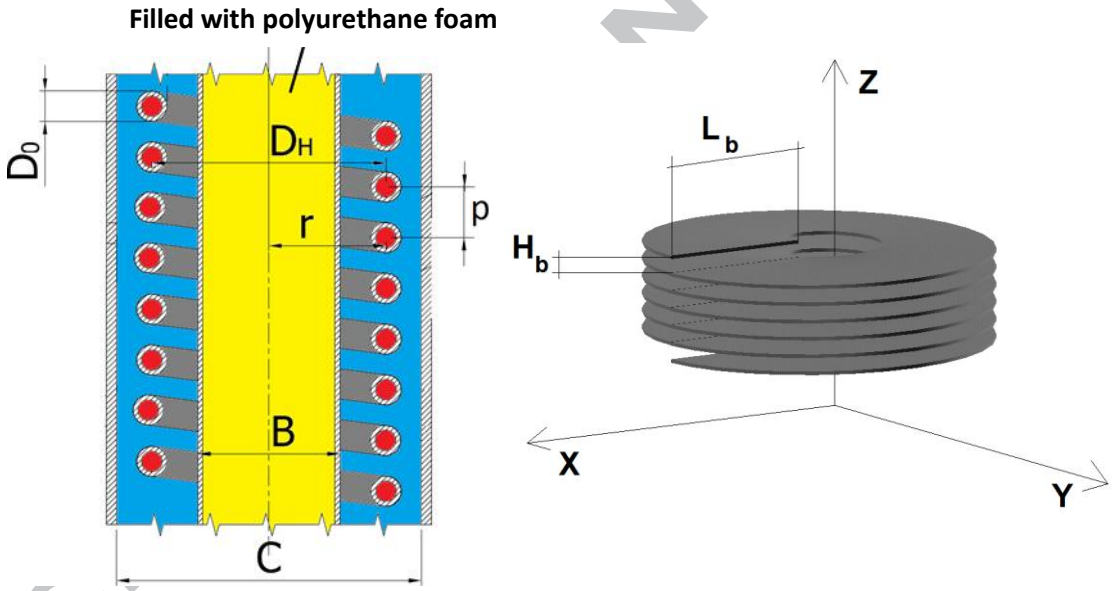

Fig. 2. Geometrical assumptions of the test module and baffle

Table 1. Geometrical characteristic of testing module

Symbol	Unit	Value
r	m	0.025
p	m	0.01
C	m	0.1
D_o	m	0.0064
D_H	m	0.05
B	m	0.032
H_b	m	0.01

L_b	m	0.034

The experiments were carried out using improved experimental test section presented in [29]. The main elements of the experimental unit were presented in Fig.3. The infrared camera (FLIR E6) was used to visualize shell wall temperature distribution. The data from the infrared camera were also used to estimate of heat loss of the assembly.

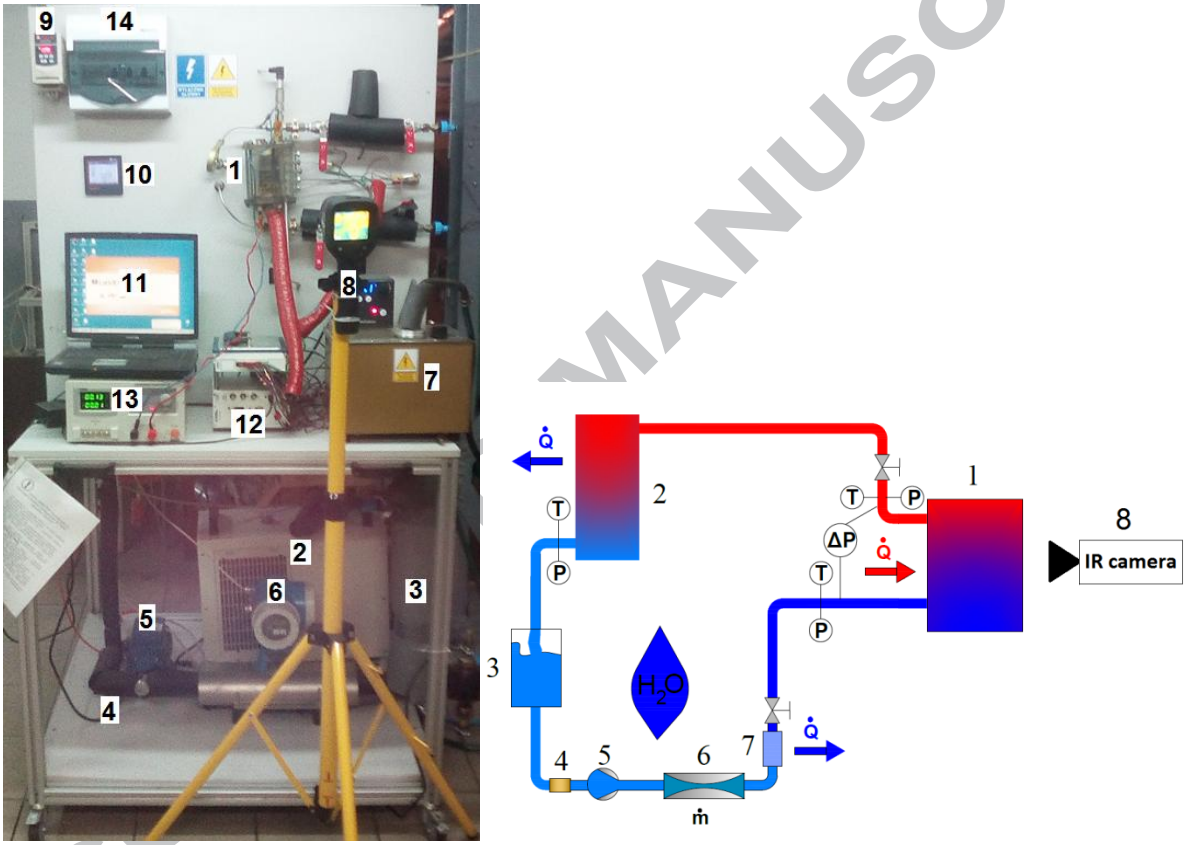

Fig. 3. Test section: 1 – test module, 2 – chiller, 3 – fluid tank, 4 – filter, 5 – gear pump, 6 – Coriolis mass flowmeter, 7 – ultra thermostatic bath,8 - infrared camera, 9- inverter, 10 - control system , 11 - PC, 12 - acquisition data system (NCXI National Instruments), 13 - DC supplier, 14 - electric switchboard

The large differences in shell wall temperature occurred during experiments. It was because of the high range of water mass flow rate as well as electric heat flux. It was one of the reasons that the infrared photos of shell were made constantly in the course of the research. To estimate heat loss all photos were scrutinized carefully.

Pressure drop measurement was carried out using the piezoelectric smart differential pressure transmitter (Siemens Sitrans P). Microprocessor control enables measurement temperature and hysteresis compensation; it also allows to provide an extended linear temporal stability. The measuring range of the transmitter is of 5–500 kPa, and the measuring accuracy is ±0.065%FS.

The wall temperature profile was usually close to logarithmic function. Due to that authors decided to assume that the average temperature difference could be calculated from logarithmic mean temperature difference (between the wall and ambient temperatures). Heat transfer coefficient for air side was calculated using eq. (6) for the vertical cylinder [31].

$$LMTD = \frac{(T_{in,shw} - T_a) - (T_{out,shw} - T_a)}{ln\left(\frac{(T_{in,shw} - T_a)}{(T_{out,shw} - T_a)}\right)} \tag{5}$$

$$Nu_{shw} = \left[0.825 + \frac{0.387 \cdot Ra^{\frac{1}{6}}}{\left[1+(0.492/Pr)^{\frac{9}{16}}\right]^{\frac{8}{27}}}\right]^2 \tag{6}$$

$$Ra = Gr \cdot Pr = \frac{\beta \cdot g \cdot {D_0}^3}{\nu^2} \cdot LMTD \cdot Pr \tag{7}$$

$$\alpha_{sw} = \frac{\mathrm{Nu} \cdot \lambda_a}{\mathrm{H}} \tag{8}$$

$$\dot{Q}_{loss} = \alpha_{sw} \cdot \pi \cdot D_{sh} \cdot H \tag{9}$$

It turned out that total heat losses were lower than 1 %. The measured uncertainty parameters are shown in Tab. 2.

Table 2. Uncertainties of selected parameters

Parameter	Operating range	Uncertainty
D_0[mm]	6.4	±0.003
m[kg/s]	0.01-0.03	±0.3%

T_w [˚C]	19-92	±1
$T_{i\text{-}o}$ [˚C]	12-50	±0.5
$T_{w,sh}$[˚C]	12-50	±1
ΔP[mbar]	2-20	±0.065%
$\dot{Q}_{el}$ [W]	100-1200W	max=±5%

The steady-state experiments were performed for three different heat exchanger configurations; reference, bottom, and top baffle geometry, as presented in Fig. 4. Plexiglas was used to create the baffles, to eliminate the fin effect on the heat transfer coefficient due to its low thermal conductivity. All materials used to fabricate the test heat exchanger module are gathered in the tab. 3

Table 3. Heat exchanger construction

Parts name	**Material**
Casing	Plexiglas (PMMA)
Baffle	PMMA
Coil	Copper
Core	Polyethylene (PE)
Heater	Kanthal

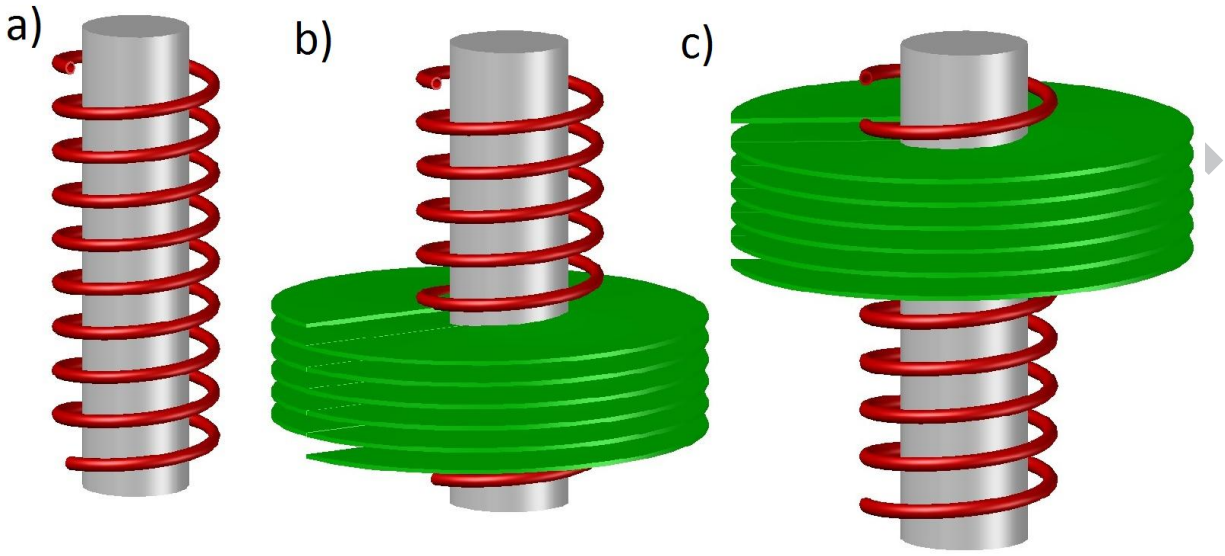

Fig. 4. View of shell side geometry configuration: a) reference geometry, b) geometry with six baffles at the bottom of the heat exchanger, c) geometry with six baffles at the top of the heat exchanger

3. Calculation methodology

The heat flux value generated in electric heater was calculated from Ohm's law, as in Eq. (10). The heat absorbed by cold water can be calculated as in equation (11).

$$\dot{Q}_{el} = U \cdot I \tag{10}$$

$$\dot{Q}_w = \dot{m}_w \cdot cp \cdot \left(T_{out} - T_{in}\right) \tag{11}$$

To account for heat losses, heat flux based on Eq. (11) was used in further analysis. Because an electric heater was used, constant heat flux density on heater surface was assumed:

$$q = \frac{\dot{Q}_w}{A_{shw}} \tag{12}$$

The local value of heat transfer coefficient was calculated as a ratio between heat flux and temperature difference (between the local temperature of coil wall surface and water temperature in the shell), see eq. (13).

$$\alpha_{sh,i} = \frac{q}{T_{shw,i} - T_{w.i}} \tag{13}$$

The Reynolds number was calculated as a function of equivalent shell diameter. Similarly as in Mianroudi et al. [3] study, following eqs. (14-17).

$$\mathrm{Re} = \frac{G \cdot De}{\mu} \tag{14}$$

$$G = \frac{\dot{m}_s}{\frac{\pi \cdot (C - B)^2}{4}} \tag{15}$$

$$De = \frac{4 \cdot V_s}{\pi \cdot (C - B) \cdot H} \tag{16}$$

$$V_s = \frac{\pi \cdot C^2}{4} \cdot H - \left[\left(\frac{\pi \cdot D_0^{\,2}}{4} \cdot L \right) + \left(\frac{\pi \cdot B^2}{4} \cdot H \right) \right] \tag{17}$$

Based on local HTC and equivalent diameter local Nusselt number was calculated (18). The average Nusselt number was calculated by integrating local values, as in Eq. (19).

$$Nu_{si} = \frac{\alpha_{si} \cdot De}{\lambda} \tag{18}$$

$$Nuav = \frac{1}{n} \cdot \int_{i=1}^{n} Nu_{si} \tag{19}$$

The calculation methodology for pressure drop was based on literature [29,30,32]. For this reason, it was decided not to repeat this information. To analyze the importance of natural

convection relative to the forced convection also the Richardson number has been taken into account as one of the pertinent parameters. This parameter was calculated directly to the equations

$$Ri = \frac{Gr}{\mathrm{Re}^2} \tag{20}$$

$$Gr = \frac{g \cdot \beta \cdot \Delta T \cdot {D_0}^3}{\nu^2} \tag{21}$$

4. Experimental results and discussion

The present study shows results of steady-state heat transfer experiments, conducted for shell coil heat exchanger in order to obtain working fluid temperatures and heat fluxes. During the experiments, ~100 experimental data points were gathered for each configuration. Resulting in over 300 experimental data on water and wall temperature distributions.

4.1 Hydraulic characteristic

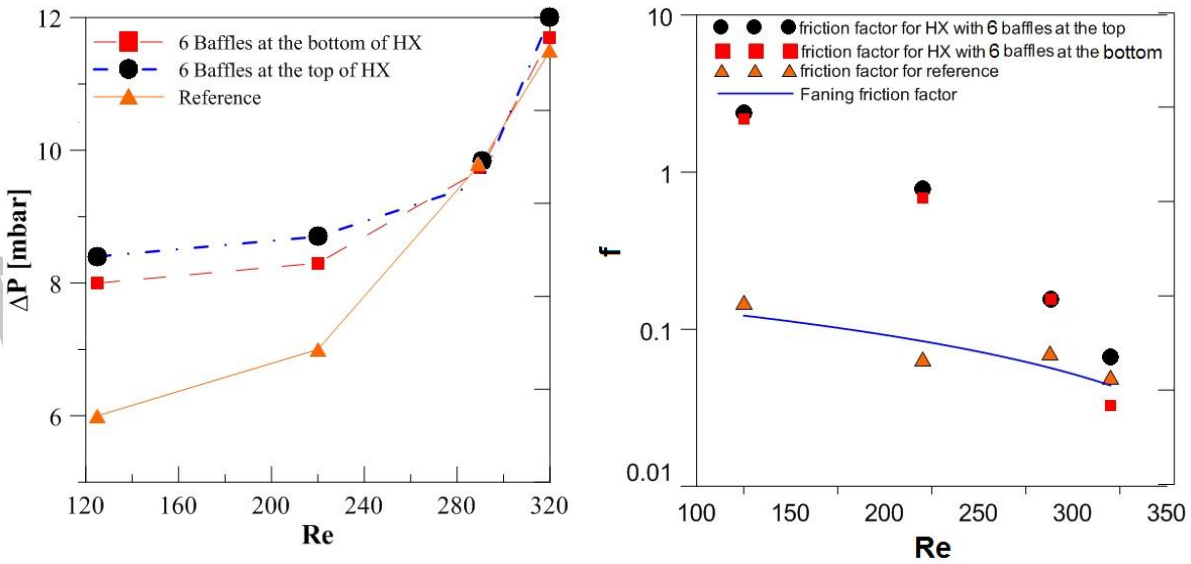

Fig. 5 Hydraulic characteristic for shell side geometry configurations: at left total pressure drops characteristic, at right friction factors vs Reynolds numbers

As can be seen in Fig.5 measured total pressure drops are very similar for all configurations presented earlier in Fig. 4. Only for small Reynolds numbers (Re<280), the differences are larger. It could be explained by the higher percentage of measurement errors in the obtained results. It had also a significant influence at friction factors coefficients. However for reference geometry experimental values of friction factor are in good fit with results calculated for smooth pipe (*f=16/Re*).

4.2 **Influence of inlet and configuration on shell temperature distribution**

The main aim of the new continuous baffle design was to enhance mixing of the working fluid at the shell of the heat exchanger and an increase of heat transfer efficiency. As is well known from the open literature there is a significant impact of inlet geometry on the flow patterns in the shell of the heat exchanger at natural and mixed convection conditions [33].

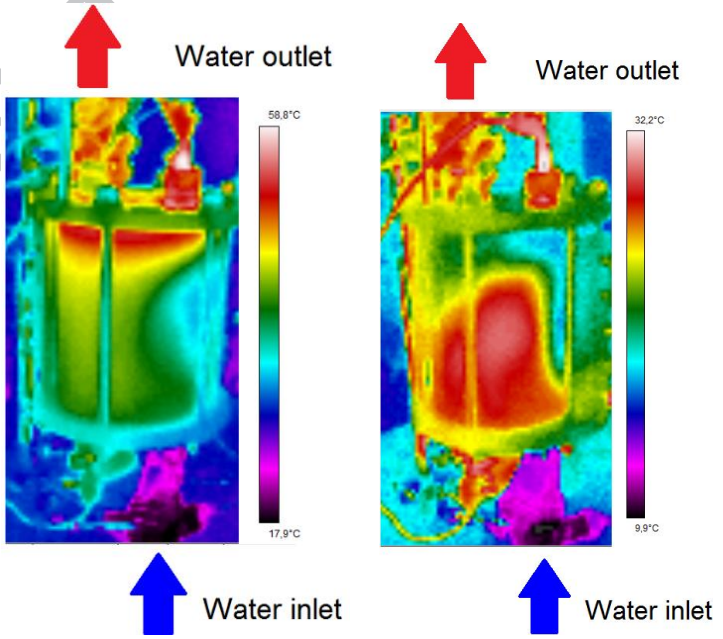

Fig. 6 Representative infrared photos of the shell wall temperature distribution for reference geometry : at left for Re=146 and Q=1100 W; at right for Re=365 and Q=1100 W

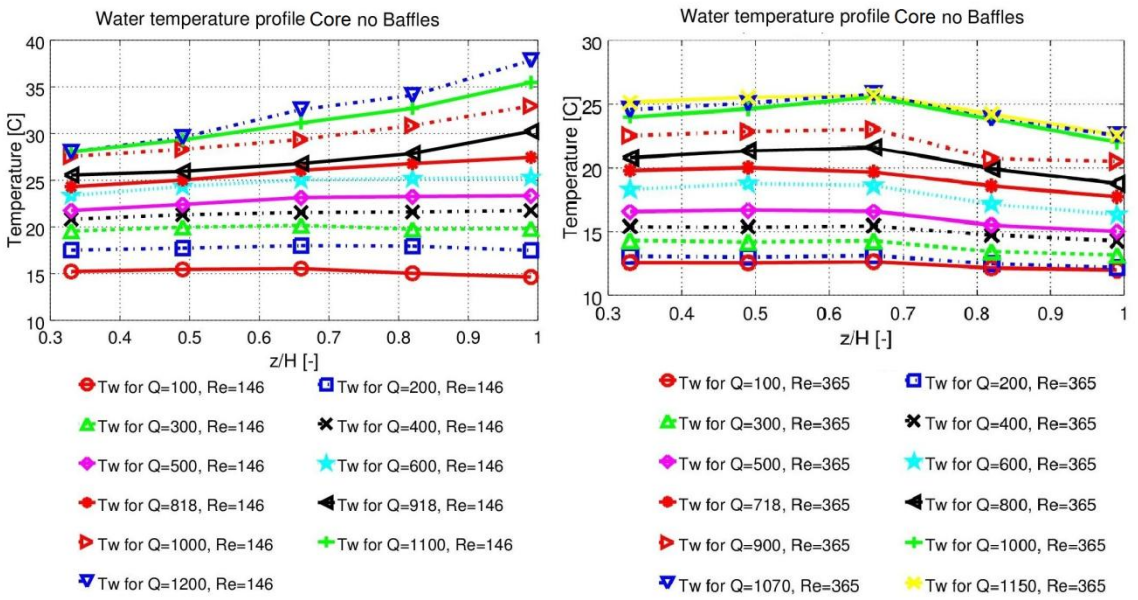

Fig 7. Water temperature profiles for constant Reynolds number - reference geometry

Similar effects can be seen in the presented study. As can be seen in representative infrared camera photos of the shell, wall temperature distribution are not uniform in case of reference geometry, see Fig.6. The presence of cold regime at the inlet of the working fluid is clearly visible. What is more, the shape of the cold regime is affected by water mass flow rate. The larger velocity of cold water can block out the hot water flow towards the outlet. This phenomenon was also confirmed by analyzing the water profile distribution, see Fig.7. In the case of the lower values of the Reynolds number, the temperature distribution is almost linear. The temperature rises along the exchanger. In the case of the larger value of the Reynolds number situation is quite opposite. The temperature rises to about half the height of the heat exchanger and then it decreases.

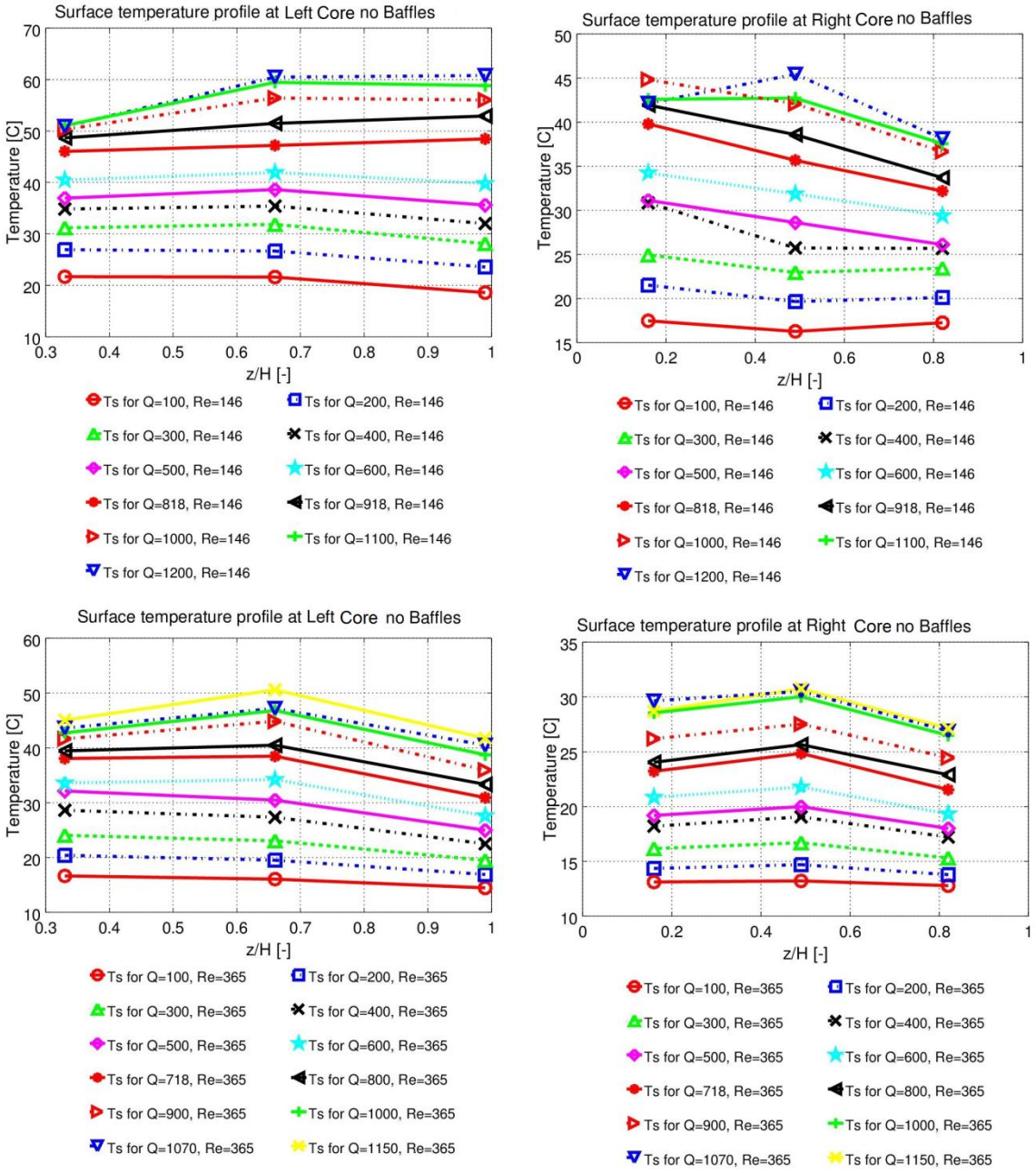

Fig 8. Wall temperature profiles for left and right side of shell coil - reference geometry

The flow distribution has a direct influence on the temperature profile of coil surface temperature distribution. It could be observed that the right side of HX the coil surface temperatures is lower than temperatures of the surface coil at the left side, see Fig.8. It could be explained by inlet influence which is more visible for larger water velocity in the shell. The situation is different for next configuration of the heat exchanger. The geometry of the

shell was modified by inserting the continuous baffle. The baffles were fastened at the bottom of the heat exchanger. The wall temperature distribution is similar at both sides of the heat exchanger. Nevertheless, the presence of hot water regime close to the center of the heat exchanger could be observed. This location of the hot area converged with the location of the end of the baffle. This effect is weaker for the larger velocity of working fluid, see Figs. 9 and 10. Also at coil surface temperature distribution, the influence of the inlet was weaker than in the case of reference geometry. Still, the profiles of temperature at left and right side were not uniform.

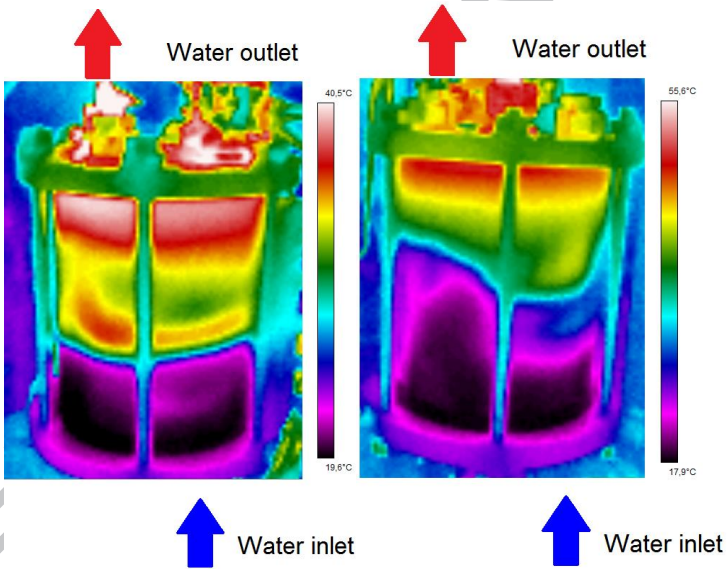

Fig 9. Representative infrared photos of the shell wall temperature distribution for HX configuration with baffle at the bottom : at left for Re=146 and Q=1100 W; at right for Re=365 and Q=1100 W

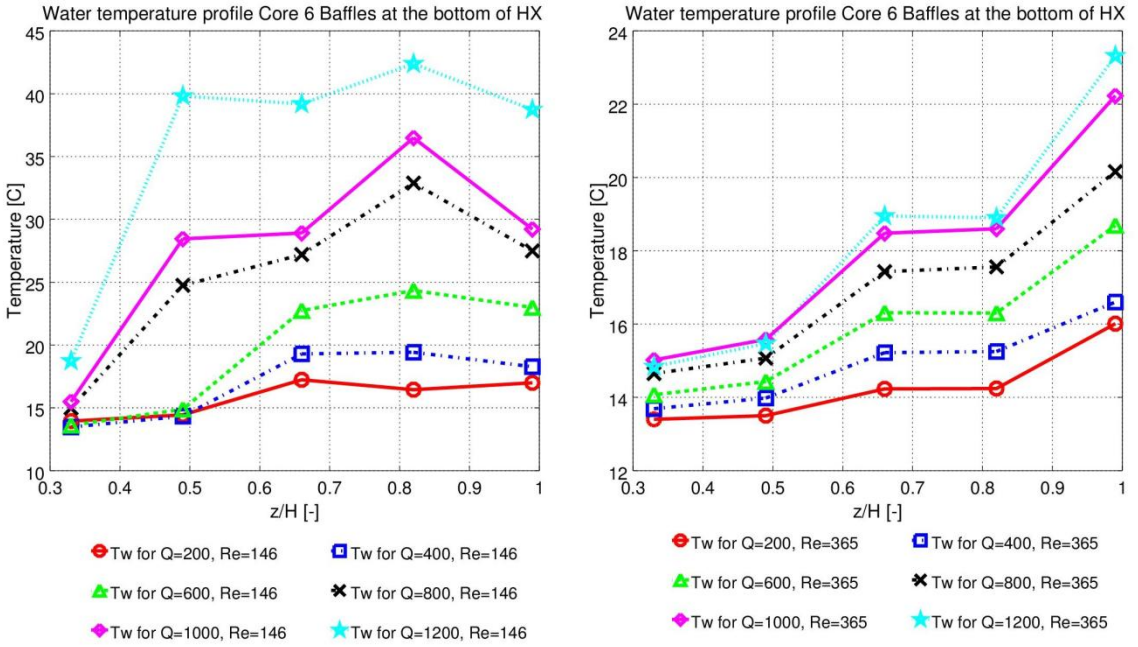

Fig 10. Water temperature profiles for a constant Reynolds number for the HX configuration with baffle at the bottom

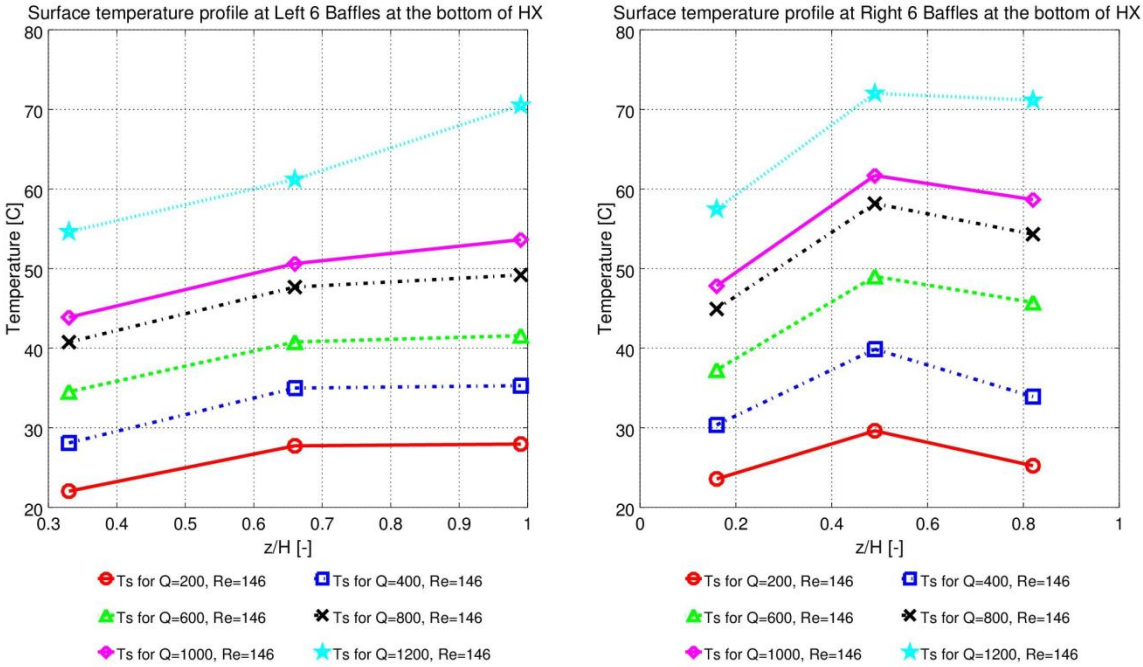

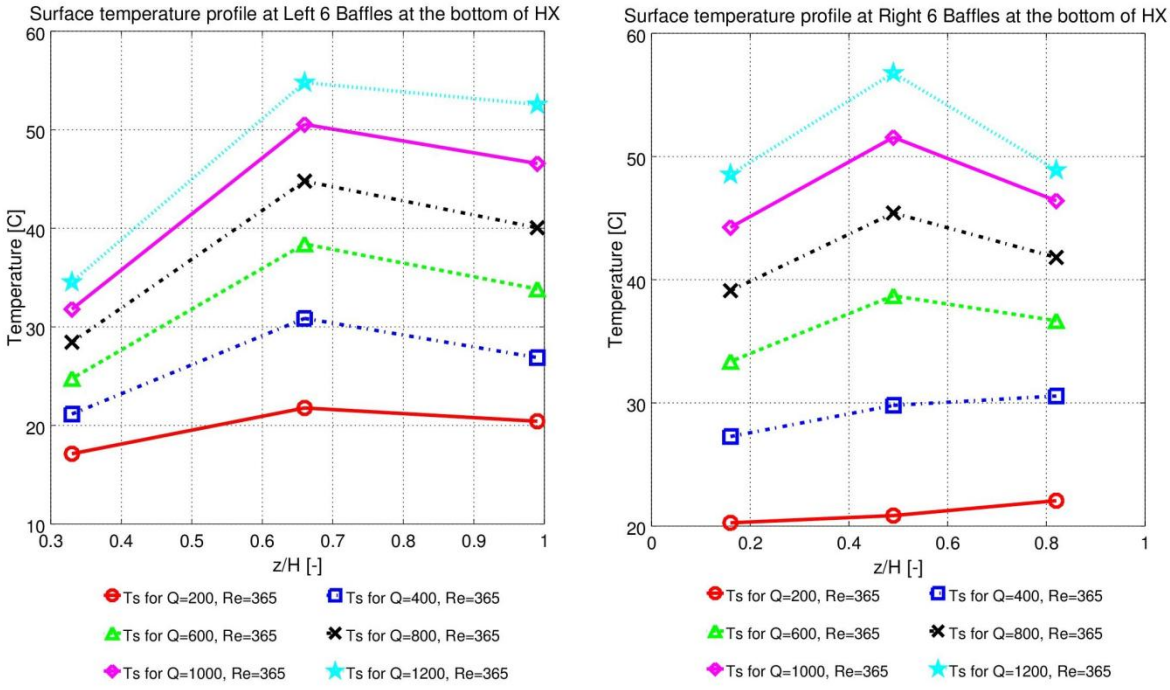

Fig 11. Wall temperature profiles for left and right side of shell coil for the HX configuration with baffle at the bottom

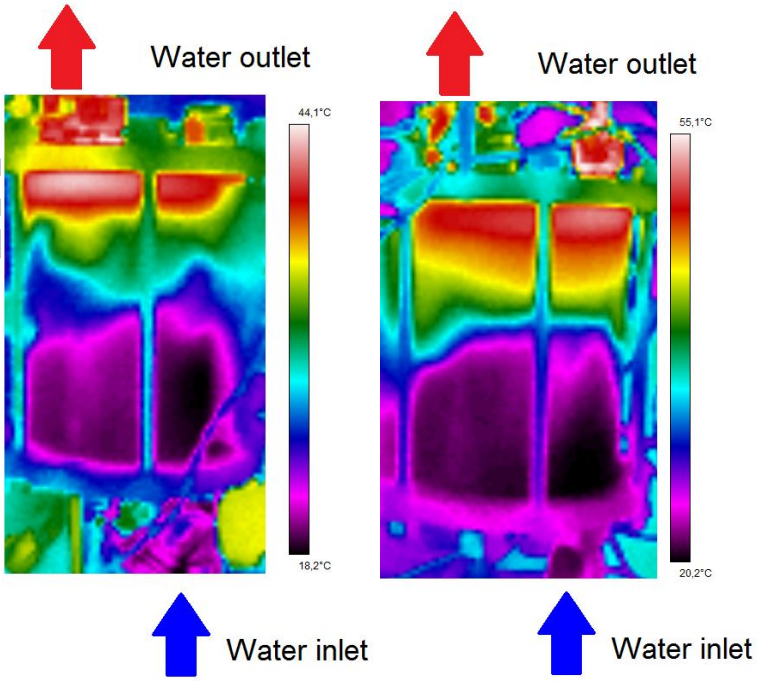

Fig 12. Representative infrared image of the shell wall temperature distribution for HX configuration with baffle at the top : at left for Re=146 and Q=1100 W; at right for Re=365 and Q=1100 W

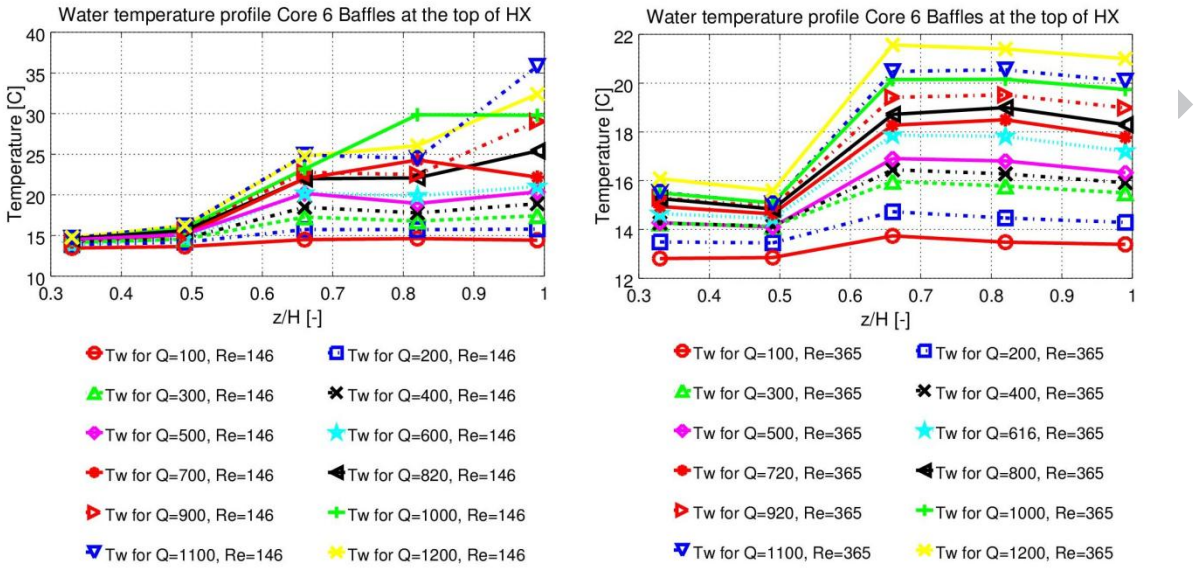

Fig 13. Water temperature profiles for constant Reynolds number for HX configuration with baffle at the top

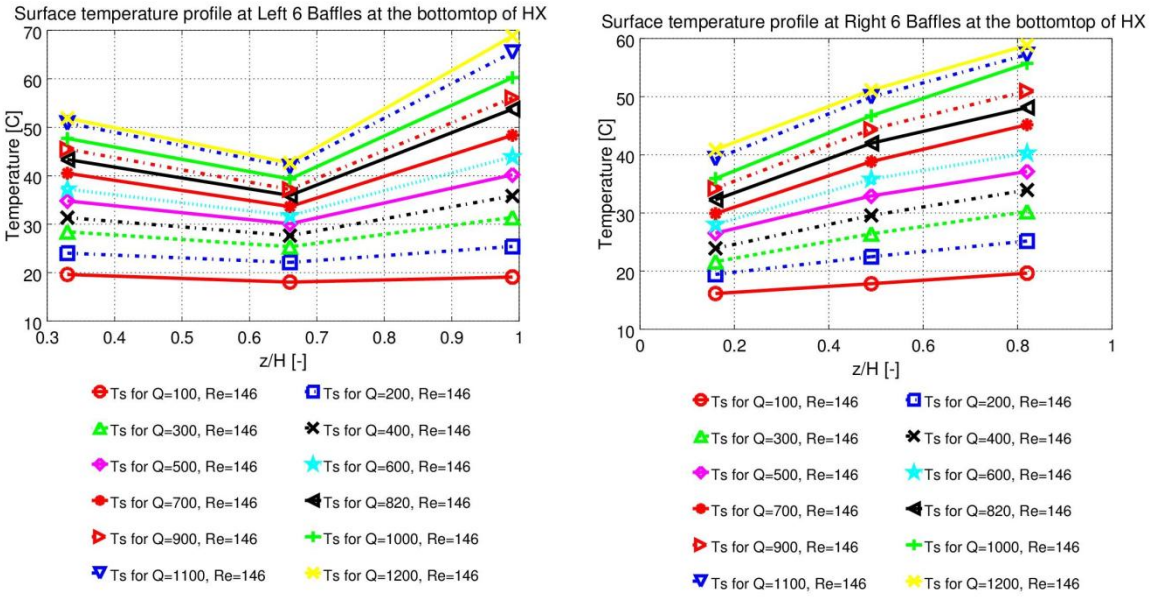

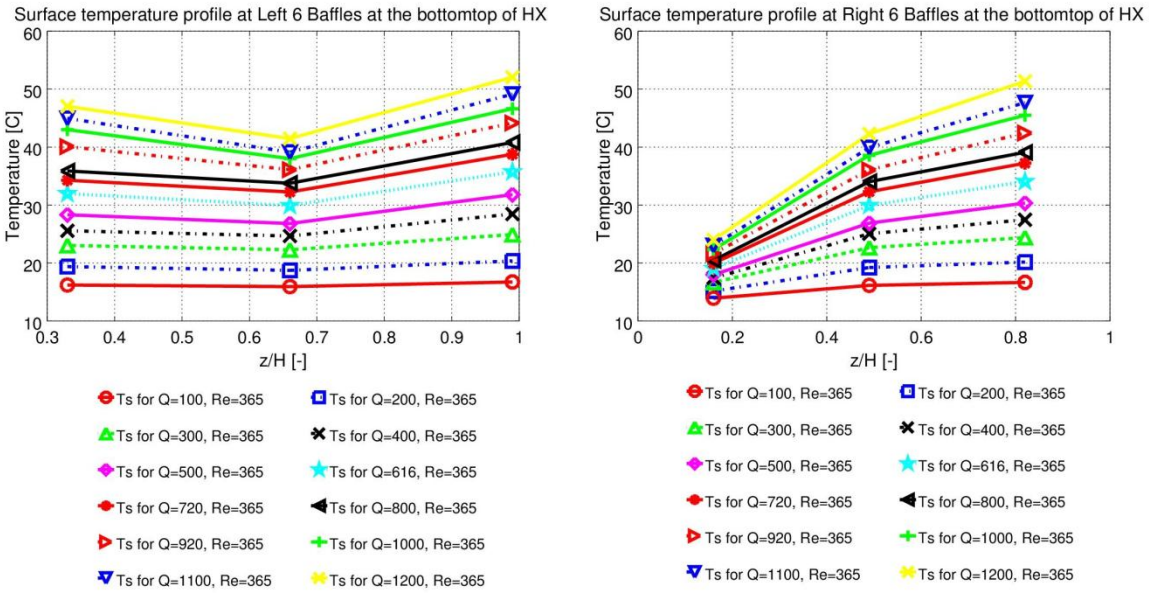

Fig 14. Wall temperature profiles for left and right side of shell coil for HX configuration with baffle at the top

In the last configuration, the baffle was fastened at the top of the heat exchanger. For that configuration, much more uniformity of wall temperature distribution was observed, see Fig.12. Neither inlet block effect or extra hot regimes in the middle of the heat exchanger were visible. The water temperature is rising along the height of the exchanger, but for larger values of the Reynolds number, the temperature profile is flatter in the middle of the heat exchanger (Fig. 13). It is worth to note that large cold surface temperature decrease close to the baffle inlet is clearly visible. This could be explained as an effect of vortex caused by the rapid change of flow direction. The visualization of flow profiles for reference geometry and geometry with the baffle at the bottom of HX was presented at Fig. 15.

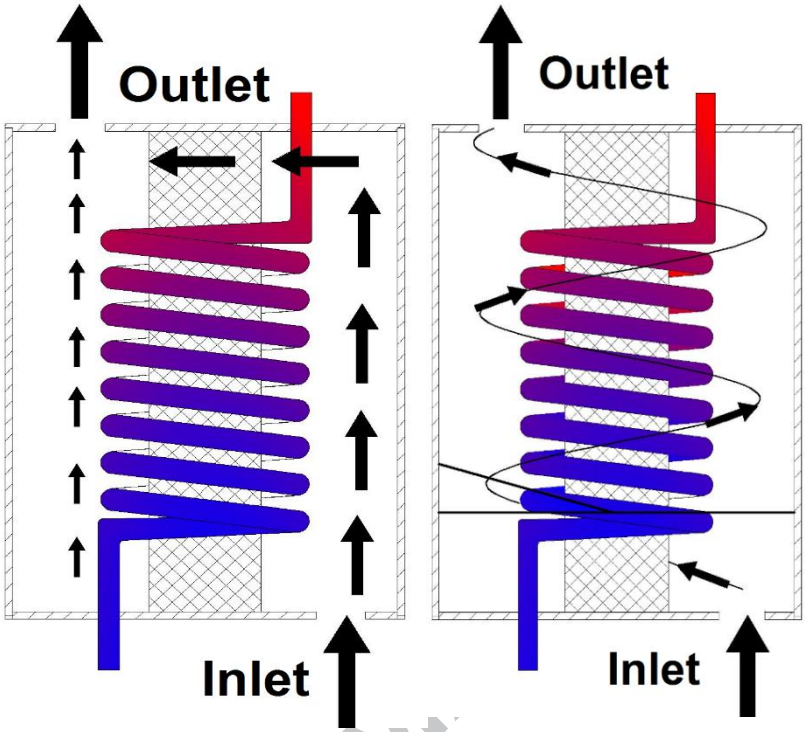

Fig. 15. Predicted flow distribution at shell side: at the left side reference geometry, at right side geometry with helical baffles

4.3 **Baffle effect on buoyancy**

Interpretation of temperature profiles can be confusing. In order to describe main heat transfer mechanism, Richardson number was used, eq. (20). Typically, the natural convection is negligible when $Ri < 0.1$, forced convection is negligible when $Ri > 10$, and neither is negligible when $0.1 < Ri < 10$ [34].

In all of the presented cases, high Richards numbers prove that natural convection mechanisms are taking the key part in heat transfer, Figs. 16-18. Only for higher flow rates corresponding to Reynolds numbers higher than 250, the influence of forced convection is visible. Baffle located at the bottom causes higher Richards number values in lover flow rates. This is an evidence of higher thermal stratification. This effect is weaker in case of baffles located at the top of the heat exchanger.

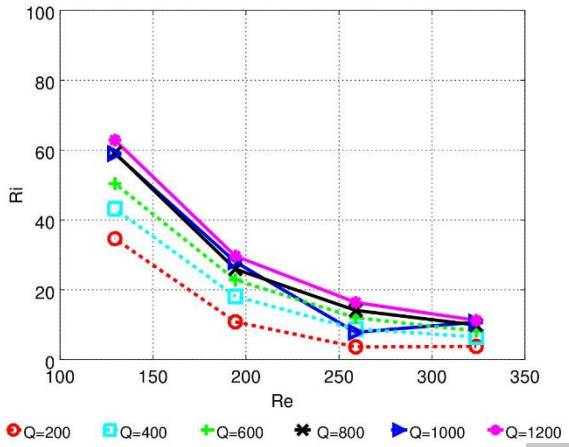

Fig. 16. Experimental values of Richardson number in function of Reynolds number for reference heat exchanger

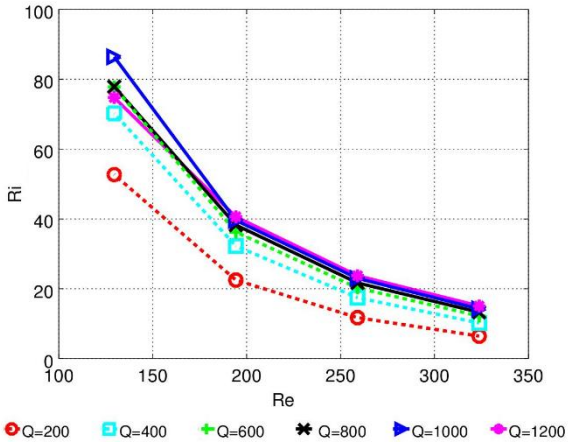

Fig. 17. Experimental values of Richardson number in function of Reynolds number for heat exchanger with baffle location at the bottom

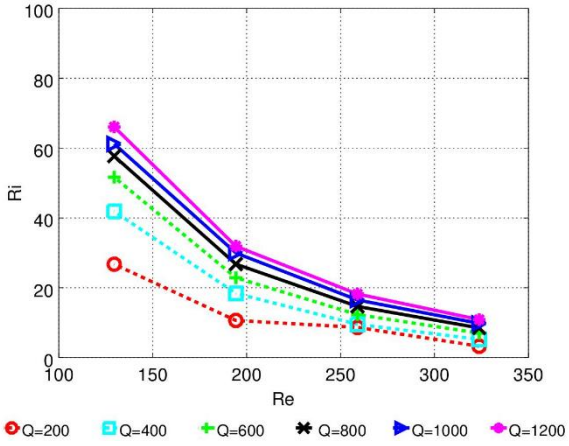

Fig. 18. Experimental values of Richardson number in function of Reynolds number for heat exchanger with baffle location at the top

The analysis shows that, due to the presence of mixed convection, natural convection has a significant effect for small values of Reynolds numbers and large values of Richard's number. Also, the baffles location has a significant influence on HX performance. It turns out that this form of continuous baffles could enhance heat transfer but rather for big values of the Richardson number (in the case of buoyancy force domination). It should be also noted that proper placement of baffles could prevent the occurrence of the dead zones in the heat exchanger, which in turn could help to avoid overheating and failure of heating elements .

4.4 **Heat transfer**

As mentioned in the previous section the geometry with continuous baffles at the top of HX affected the flow causing almost uniform water and coil surface temperature. Neither inlet block effect or extra hot regimes in the middle of the heat exchanger were visible for that case. Baffles increase the flow pathway significantly, what can be observed as a higher HTC for lower fluid flow rates. As can be seen when comparing Figs. 18-21 average Nusselt numbers for baffled geometry are 10- 25% higher than values for reference heat exchanger, Fig 18.

For baffle configuration at the bottom of HX, despite the fact that the influence of the inlet was weaker than in the case of reference geometry, non-uniform temperature profiles (water and coil surface) were observed. Nusselt number values yield that heat transfer effectiveness is lower than in previous configurations. The heat transfer enhancement, compared to reference geometry, is observed only at small values of Reynolds number. In this regime, average Nusselt numbers are ~ 10% higher than values for a reference type.

Undoubtedly, this form of continuous baffles could enhance heat transfer for mixed and natural convection conditions. It should also be noted that the location of baffles is the key parameter. The best results were obtained for the heat exchanger with baffles placed at the top. In authors opinion, the performance differences between heat exchanger configurations could be explained by the difference of local fluid velocity. At the top of the heat exchanger, the average temperature difference between coil surface and water are much smaller compared to the bottom. So the mixing effect should be more visible in that regime. However, baffles should increase mixing of water in both configurations. So theoretically they should enhance heat transfer in both configurations. However obtained results (for configuration with baffle location at the bottom) shown that the water was mixing in the spaces between the baffles but at the end, its track was curved towards the outlet. This shortens water contact with the heat exchange surface and creates nonuniform wall temperatures profile .The situation was very different in case of baffles located at the top of HX.

`

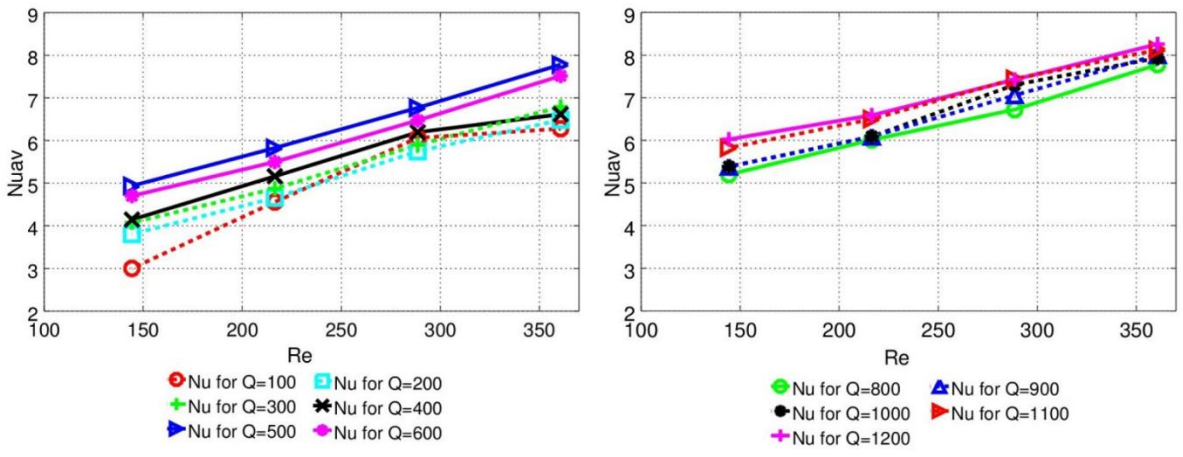

Fig. 19. The average Nusselt number for constant heat flux in function of Reynolds number for reference geometry.

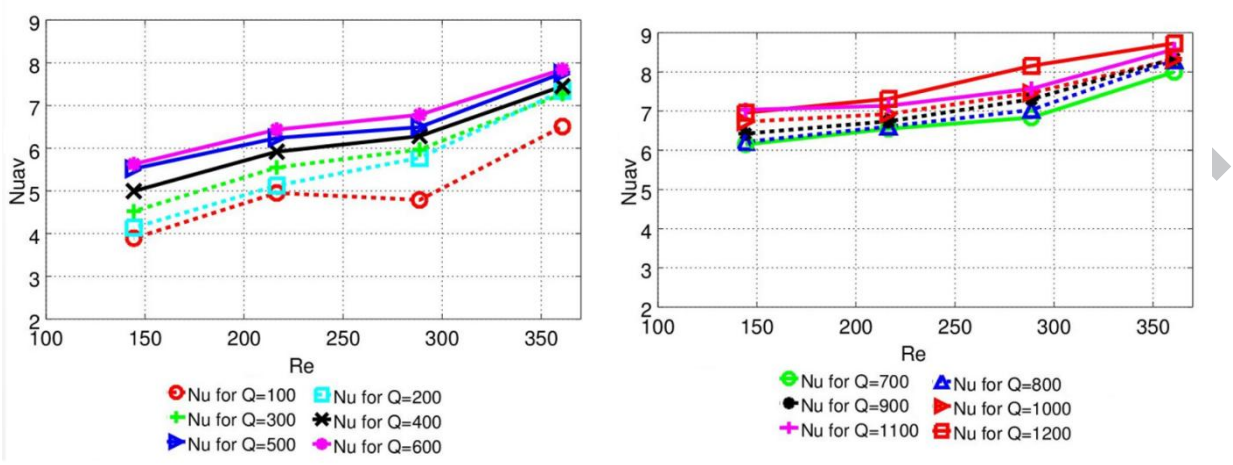

Fig. 20 The average Nusselt number for constant heat flux in Function of Reynolds number for HX configuration with baffle location at the top.

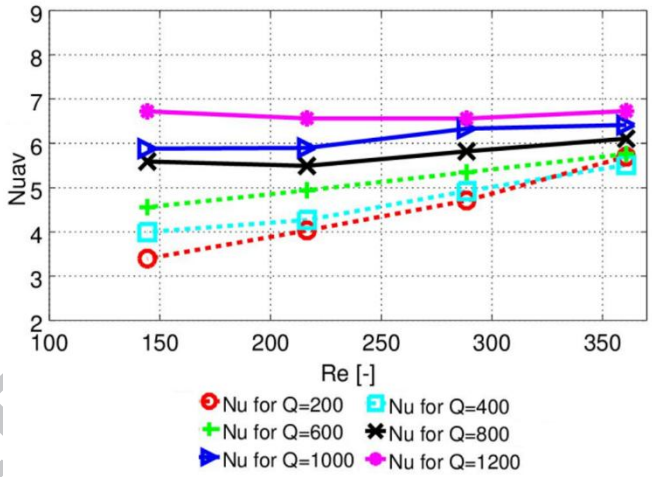

Fig. 21 The average Nusselt number for constant heat flux, in function of Reynolds number for HX configuration with baffle location at the bottom.

4.5 Experimental data validation

Experimental data were compared with selected correlations presented in the introduction, see Fig. 21. The correlations are developed based on non-dimensional numbers, with equivalent diameter as a characteristic length. As in proposed research the geometrical dimensions of the coil and casing do not change, the correlations can't follow the data trend accurately. The varying parameter was water flow rate and temperature, for geometries with

different baffle location. The comparison shows that only the Mahdi [28] correlation gives predictions that partly predict experimental data within 30% error band. Due to that fact authors proposed their own experimental correlation, in which experimental HTC depends on dimensionless Grashoff and Dean numbers. Correlation also includes Prandtl number accounting for the water properties shift with temperature. Experimental coefficients describing baffle geometry were based on data best fit. Geometrical HX parameters used in eq.(21) are presented in Fig. 2 and listed in Tab.1.

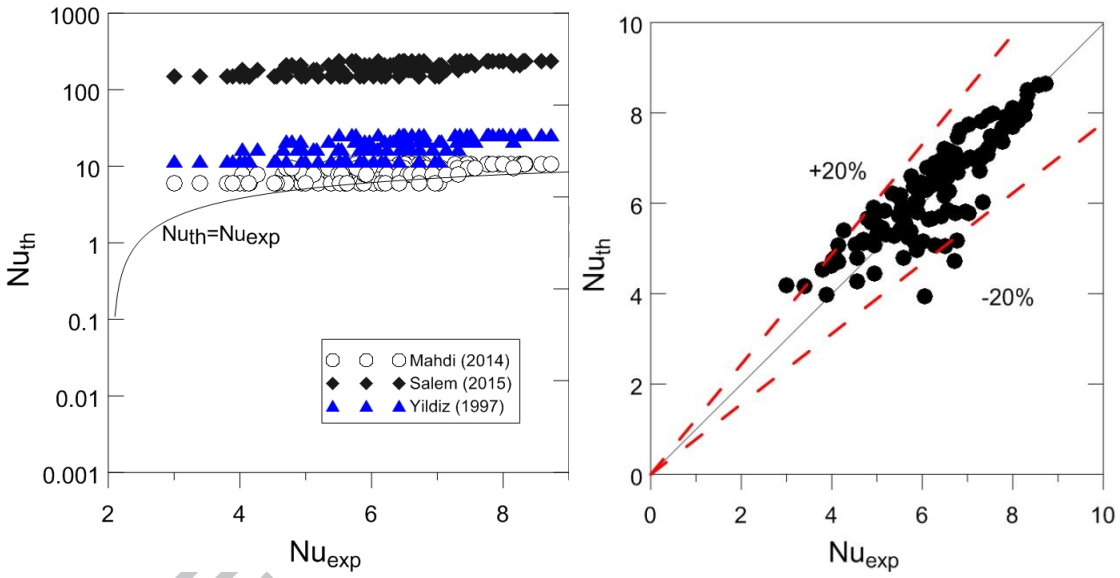

Fig. 22 Comparision experimental Nusselt number: at left with correlation from literature, at right with own experimental correlation

$$Nu = 4.52 \cdot 10^{-3} \cdot (Gr \cdot De \cdot \mathrm{Pr})^{m} \cdot \left[\frac{\frac{A_{sh}}{A_b}}{N \cdot \frac{H}{L_b}}\right]^{n} \qquad (21)$$

where m = 0.357 and n=0 for N = 0; m = 0.357 and $n = \frac{1}{N^2}$ for N = 6 at bottom; m = 0.371 and $n = \frac{1}{N^2}$ for N = 6 at top and $A_b = H_b * L_b$.

As presented in Tab. 3 proposed correlation (eq. 21) achieves absolute deviation less than 6% for all presented data.

Table 3. The Relative error between predicted and experimental Nusselt numbers

Data set	MAD [%]	% of data within +/- 20%
SCHX Core	0,73	93,19
SCHX Baffle Bottom	5,61	96
SCHX Baffle Top	1,91	98

In order to emphasize the impact of the presented modification of flow geometry in the shell coil HX, the results of presented research were compared with the literature results in the form of a performance comparative graph. The performance factor was calculated as below (eq. 22)

$$PF = \frac{\frac{Nu}{Nu_r}}{\left(\frac{f}{f_r}\right)^{0.1667}} \tag{22}$$

The results of comparison were shown in fig 23.

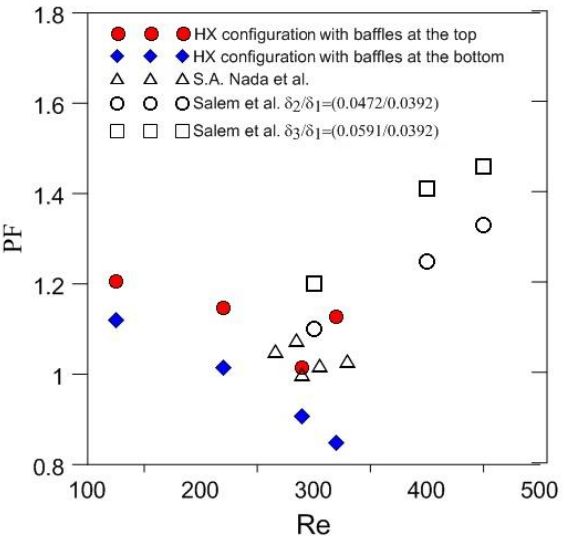

Fig. 23 Performance analysis of new continuous core-baffle geometry for selected series of data (Q=400) compared to the results available in the literature.

The performance analysis confirms the possibility of intensifying heat exchange in the shell coil heat exchanger by using of new continuous core-baffle geometry. However satisfactory heat transfer enhancement was obtained rather for low values of Reynolds number (Re<300). What is more important that this flow regime is generally characterized by small values of

heat transfers coefficients. In flow regime with domination of forced convection influences at heat transfer, it is worth to consider other enhancement methods such as by changing the shape parameters of the coil.

5. Conclusions

The article presents passive heat transfer enhancement method in the form of new continuous baffles to increase the energy efficiency of the shell coil heat exchanger. Conducted literature review shows a lot of interest with the enhancement techniques for all types of heat exchanger constructions. In case of shell coil heat exchangers, most of the research is focused on intensification of coil side heat transfer coefficient. So there is still much to do in order to increase the efficiency of this type of heat exchangers. In present study authors concentrated on the possibility to use a new continuous baffle geometry. Attention was also focused on dead zones as the effect of inlet/outlet flow parameters and baffle configurations.

This work shows that, due to the presence of mixed convection, natural convection has a significant effect for small values of Reynolds numbers and large values of Richard's number. Also, the baffles location has a significant influence on HX performance. It turns out that this form of continuous baffles could enhance heat transfer but rather for big values of the Richardson number (in the case of buoyancy force domination). It should be also noted that proper placement of baffles could prevent the occurrence of the dead zones in the heat exchanger, which in turn could help to avoid overheating and failure of heating elements.

Selected literature predictions overestimate heat transfer coefficients at shell side of shell coil heat exchanger. The comparison shows that only the Mahdi [28] correlation partly

predicts experimental data within 30% error band. Due to that fact authors proposed their own experimental correlation, in which experimental HTC depends on dimensionless Grashoff and Dean numbers. Presented simple experimental correlation gives a satisfactory compliance with experimental results. It should be noted that the correlation can be applied for all of the presented heat exchanger configurations.

The performance analysis confirms the possibility of heat transfer enhancement in the shell coil heat exchanger by using of new continuous core-baffle geometry. However this enhancement method is rather dedicated to mixed convection conditions.

Literature

[1] S.A. Berger, L. Talbot, L.S. Yao, Flow in curved pipes, Annu. Rev. Fluid Mech. 15 (1983) 461–512.

[2] T.A. Pimenta, J. Campos, Friction losses of Newtonian and non-Newtonian fluids flowing in laminar regime in a helical coil, Exp. Therm. Fluid Sci. 36 (2012) 194–204.

[3] N. Ghorbani Mianroudi, M. Gorji, H. Taherian, Experimental Study of Mixed Convection Shell-and-Coil Heat Exchanger, (2008) 129–135. http://dx.doi.org/10.1115/HT2008-56504.

[4] R.K. Patil, B.W. Shende, P.K. Ghosh, DESIGNING A HELICAL-COIL HEAT EXCHANGER., Chem. Eng. (New York). 89 (1982) 85–88.

[5] A. Zachár, Analysis of coiled-tube heat exchangers to improve heat transfer rate with spirally corrugated wall, Int. J. Heat Mass Transf. 53 (2010) 3928–3939.

[6] T. Muszynski, R. Andrzejczyk, Heat transfer characteristics of hybrid microjet - Microchannel cooling module, Appl. Therm. Eng. 93 (2016) 1360–1366. doi:10.1016/j.applthermaleng.2015.08.085.

[7] T. Muszynski, S.M. Koziel, Parametric study of fluid flow and heat transfer over louvered fins of air heat pump evaporator, Arch. Thermodyn. 37 (2016) 45–62. doi:10.1515/aoter-2016-0019.

[8] S. Brückner, S. Liu, L. Miró, M. Radspieler, L.F. Cabeza, E. Lävemann, Industrial waste heat recovery technologies: An economic analysis of heat transformation technologies, Appl. Energy. 151 (2015) 157–167. doi:10.1016/j.apenergy.2015.01.147.

[9] D. Mikielewicz, R. Andrzejczyk, B. Jakubowska, J. Mikielewicz, Analytical Model With Nonadiabatic Effects for Pressure Drop and Heat Transfer During Boiling and Condensation Flows in Conventional Channels and Minichannels, Heat Transf. Eng. 37 (2016) 1158–1171.

[10] T. Bohdal, H. Charun, M. Sikora, Empirical study of heterogeneous refrigerant condensation in pipe minichannels, Int. J. Refrig. 59 (2015) 210–223. doi:10.1016/j.ijrefrig.2015.07.002.

[11] T. Muszynski, R. Andrzejczyk, C.A. Dorao, Detailed experimental investigations on frictional pressure drop of R134a during flow boiling in 5 mm diameter channel: The influence of acceleration pressure drop component, Int. J. Refrig. 82 (2017). doi:10.1016/j.ijrefrig.2017.05.029.

[12] R. Andrzejczyk, T. Muszynski, C.A. Dorao, Experimental investigations on adiabatic frictional pressure drops of R134a during flow in 5 mm diameter channel, Exp. Therm. Fluid Sci. 83 (2017) 78–87. doi:10.1016/j.expthermflusci.2016.12.016.

[13] R.A. Białecki, T. Burczyński, A. Długosz, W. Kuś, Z. Ostrowski, Evolutionary shape optimization of thermoelastic bodies exchanging heat by convection and radiation, Comput. Methods Appl. Mech. Eng. 194 (2005) 1839–1859. doi:10.1016/j.cma.2004.07.004.

[14] W.P. Adamczyk, P. Kozołub, G. Węcel, A. Klimanek, R.A. Białecki, T. Czakiert, Modeling oxy-fuel combustion in a 3D circulating fluidized bed using the hybrid Euler–Lagrange approach, Appl. Therm. Eng. 71 (2014) 266–275. doi:10.1016/j.applthermaleng.2014.06.063.

[15] T. Muszynski, Design And Experimental Investigations Of A Cylindrical Microjet Heat Exchanger For Waste Heat Recovery Systems, Appl. Therm. Eng. (2017). doi:10.1016/j.applthermaleng.2017.01.021.

[16] S. Liu, M. Sakr, A comprehensive review on passive heat transfer enhancements in pipe exchangers, Renew. Sustain. Energy Rev. 19 (2013) 64–81.

[17] A. Bartwal, A. Gautam, M. Kumar, C.K. Mangrulkar, S. Chamoli, Thermal performance intensification of a circular heat exchanger tube integrated with compound circular ring–metal wire net inserts, Chem. Eng. Process. Process Intensif. 124 (2018) 50–70.

[18] S. Chamoli, R. Lu, P. Yu, Thermal characteristic of a turbulent flow through a circular tube fitted with perforated vortex generator inserts, Appl. Therm. Eng. 121 (2017) 1117–1134.

[19] N. Acharya, M. Sen, H.-C. Chang, Analysis of heat transfer enhancement in coiled-tube heat exchangers, Int. J. Heat Mass Transf. 44 (2001) 3189–3199. doi:10.1016/S0017-9310(01)00002-3.

[20] P. Naphon, Thermal performance and pressure drop of the helical-coil heat exchangers with and without helically crimped fins, Int. Commun. Heat Mass Transf. 34 (2007) 321–330. doi:10.1016/j.icheatmasstransfer.2006.11.009.

[21] C. Yildiz, Y. Bíçer, D. Pehlívan, Influence of fluid rotation on the heat transfer and pressure drop in double-pipe heat exchangers, Appl. Energy. 54 (1996) 49–56. doi:10.1016/0306-2619(95)00070-4.

[22] C. Yildiz, Y. Biçer, D. Pehlivan, Heat transfer and pressure drop in a heat exchanger with a helical pipe containing inside springs, Energy Convers. Manag. 38 (1997) 619–624. doi:10.1016/S0196-8904(96)00040-4.

[23] A.J.K. Thomas, R.C. Bindeesh, N.S. Thomas, P. Unaira, K.B. Radhakrishnan, Experimental Investigation on Heat Transfer Augmentation in Helical Coil Heat Exchanger Using Wire Coil/Spring Inserts, Imp. J. Interdiscip. Res. 2 (2016).

[24] D. Panahi, K. Zamzamian, Heat transfer enhancement of shell-and-coiled tube heat exchanger utilizing helical wire turbulator, Appl. Therm. Eng. 115 (2017) 607–615. doi:10.1016/j.applthermaleng.2016.12.128.

[25] J. Avina, The modeling of a natural convection heat exchanger in a solar domestic hot water system, University of Wisconsin--Madison, 1995.

[26] R. Kharat, N. Bhardwaj, R.S. Jha, Development of heat transfer coefficient correlation for concentric helical coil heat exchanger, Int. J. Therm. Sci. 48 (2009) 2300–2308.

[27] M.R. Salem, K.M. Elshazly, R.Y. Sakr, R.K. Ali, Effect of Coil Torsion on Heat Transfer and Pressure Drop Characteristics of Shell and Coil Heat Exchanger, J.

Therm. Sci. Eng. Appl. 8 (2015) 11015. doi:10.1115/1.4030732.

[28] Q.S. Mahdi, L.D.S.A. Fattah, Experimental and Numerical Investigation to Evaluate the Performance of Helical Coiled Tube Heat Exchanger, J. Eng. Dev. 18 (2014).

[29] R. Andrzejczyk, T. Muszynski, Thermodynamic and geometrical characteristics of mixed convection heat transfer in the shell and coil tube heat exchanger with baffles, Appl. Therm. Eng. 121 (2017) 115–125. doi:10.1016/j.applthermaleng.2017.04.053.

[30] R. Andrzejczyk, T. Muszynski, Performance Analyses Of Helical Coil Heat Exchangers. The Effect Of External Coil Surface Modification On Heat Exchanger Effectiveness, Arch. Thermodyn. (2016). doi:AOT-00010-2016-04.

[31] Y.A. Cengel, Introduction to thermodynamics and heat transfer, McGraw-Hill New York, 1997.

[32] G.F. Hewitt, G.L. Shires, T.R. Bott, Process heat transfer, CRC press Boca Raton, FL, 1994.

[33] L.J. Shah, S. Furbo, Entrance effects in solar storage tanks, Sol. Energy. 75 (2003) 337–348.

[34] H.D.I. Abarbanel, D.D. Holm, J.E. Marsden, T. Ratiu, Richardson Number Criterion for the Nonlinear Stability of Three-Dimensional Stratified Flow, Phys. Rev. Lett. 52 (1984) 2352–2355. doi:10.1103/PhysRevLett.52.2352.

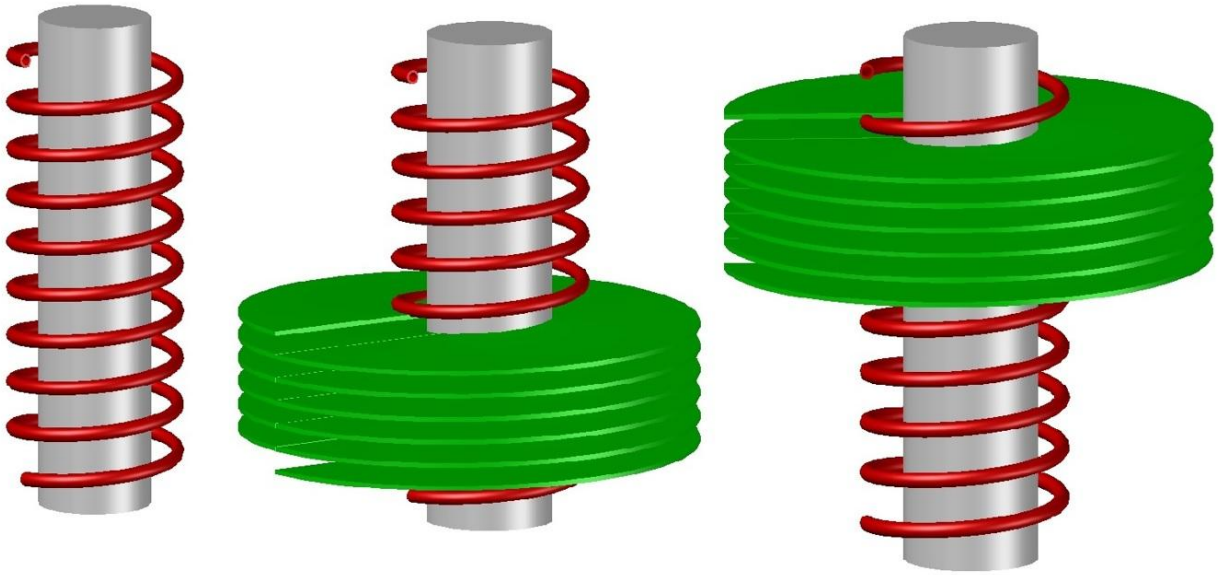

Fig. Tested heat exchanger configurations

Highlights

- **The effect of continuous baffle configuration on HX performance was investigated**
- **The influence of water mass flow and heat flux on the HTC was presented**
- **Experimental correlation for investigated configurations was developed**